Article ID: 1003－6326(2004)04－0779－06

Mechanism of stress aging in Al-Cu(-Mg-Ag) alloys①

CHEN Da-qin(陈大钦), ZHENG Zi-qiao(郑子樵), LI Shi-chen(李世晨), CHEN Zhi-guo(陈志国)
(School of Materials Science and Engineering, Central South University, Changsha 410083, China)

Abstract: The effect of stress aging on the nucleation and growth of precipitates in Al-3.88% Cu and Al-3.87% Cu-0.56% Mg-0.56% Ag alloys was investigated by electric resistivity measurement and transmission electron microscopy observation. The results indicate that external stress promotes the formation of clusters of solute atoms or GP zones, but retards the growth of θ′ and Ω phases. A critical phenomenon that the microstructural evolution will be modified at a certain external extress value is found in Al-Cu-Mg-Ag alloy. The applied external stress during aging induces preferentially oriented precipitations of θ′ and Ω in Al-Cu and Al-Cu-Mg-Ag alloys, respectively. The origin of stress-induced orientation effect is understood by analyzing interaction between external stress and misfit strain by Eshelby elastic inclusion theory.

Key words: aluminium alloy; stress aging; stress-induced orientation effect; misfit strain; nucleation; growth
CLC number: TG 166.3 **Document code:** A

1 INTRODUCTION

The hardening effect of aging-hardenable alloys is considerably determined by the species, quantity, shape, size, distribution and orientation of precipitates formed by aging. Therefore, it is critical to modify and control microstructural evolution finely during phase transformation in the field of materials science and engineering. Some research conclusions[1-9] showed that precipitation process could be modified dramastically by using a coupling of the applied elastic stress and temperature during aging (named as stress aging), which was helpful to modify and control the microstructural characteristics, and, finally, to improve the mechanical properties of materials.

Stress aging technology has been utilized in some aluminium alloys in the past few years[2-6]. For example, Hosford and Agrawal[2] studied the stress-induced orientation effect during stress aging in Al-Cu binary alloy. Eto et al[3] demonstrated that stress-induced orientation effect was initiated and determined during nucleation stage by two-step aging technology, which was supported by computer simulation results of Li and Chen[10]. Skrotzki et al[5] found that there were threshhold values of the external stress up to which the formation of prerferentially oriented precipitation could occur in the tensile-stress-aged specimens of Al-Cu and Al-Cu-Mg-Ag. Later, Zhu et al[6] systematically studied stress aging process for Al-Cu and suggested that the stress-induced orientation effect depended on the applied stress, temperature, alloy composition and aging time.

The above works were mostly focused on the experimental observation and correlated studies of stress-induced orientation effect in simple alloys. They did not involve to analyze the effect of external stress on kinetic process and the mechanism of stress-induced orientation effect deeply. In this paper, electrical resistivity measurement and transmission electron microscopy observation are coupled to investigate the effect of external stress on nucleation and growth of precipitates in Al-Cu and Al-Cu-Mg-Ag alloys. Moreover, the origin of stress-induced orientation effect is discussed through Eshelby elastic inclusion theory.

2 EXPERIMENTAL

Two alloys were used in this study and their compositions were Al-3.88% Cu and Al-3.87% Cu-0.56% Mg-0.56% Ag (mass fraction), respectively. Samples were solution treated at (520±3) ℃ for 1 h and then quenched into water rapidly. The quenched samples should be put into furnace as quickly as possible in order to prevent from natural aging and the stress must be applied before artificial aging. Resistivity was measured using two-bridge electric-resistivity method. Thin foil specimens for TEM were prepared in a twin jet electro-polisher using a solution of nitric acid and methanol (1∶3 in volume fraction) at about －30 ℃. After polishing, Ag-containing specimens were dipped in a solution of 5% nitric acid in H_2O to remove the redeposited Ag from the elec-

① **Foundation item:** Project(50271084) supported by the National Natural Science Foundation of China
Received date: 2003－12－05; **Accepted date:** 2004－02－25
Correspondence: CHEN Da-qin, Tel: +86-731-8830270; E-Mail: s-maloy@mail.csu.edu.cn

trolyte. Microstructures were observed in a H-800 electron microscope.

3 RESULTS AND DISCUSSION

Fig. 1 shows the variation of relative resistivity of the Al-Cu binary alloy aged at 180 ℃ with respect to aging time during stress aging. Four curves correspond to different applied stresses. It is well known that electrical resistivity is sensitive to a number of microstructural factors such as vacancy concentration, solute concentration in the matrix, precipitate (or cluster) size and its volume fraction. When the size of solute atoms arranged heterogeneously (GP zones, clusters) in solid solution is sized in a nanometer scale, they can scatter electrons strongly and result in increased resistivity since their size is close to the electron wave. The kinetic process of aging is different at low temperature from that at elevated temperature at which the coherent or semi-coherent metastable phases (for instance, θ'' or θ' phase in Al-Cu binary) are directly precipitated from solid solution because of more active diffusion of atoms . Therefore, electrical resistivity decreases in the beginning of elevated temperature[11, 12]. As can be seen in Fig. 1, it is found that electical resistivity decreases monotonically, implying that there are no GP zones exist. This result can be explained by considering the active diffusion of atoms at 180 ℃. Under this condition, GP zones are dissolved or transformed to θ'' or θ' phase so quickly that they can not be detected by resistivity method in a short time.

Moreover, the resistivity of stress aging is relatively higher than that under T 6 condition in different time. Since the yield strength of Al-Cu binary in solid solution is about 120 MPa[9], which is higher than that of experiment used, the dislocation cannot be introduced by elasticdif- stress. As mentioned above, resistivity is sensitive to the content of solute atoms and heterogeneous clusters in Al-Cu binary alloy and most clusters are dissolved or transformed to θ''-phases or θ'-phases at 180 ℃ in a short time, so under these conditions, it can be concluded that random Cu atoms in stress aging are much more than those of T6 condition, which means the precipitation and growth of θ-phases or θ'-phases are retarded by external stress. After a period of time of precipitation, conherent or semi-conherent metastable phases are precipitated slowly and Ostwald ripening occur, which makes resistivity stable.

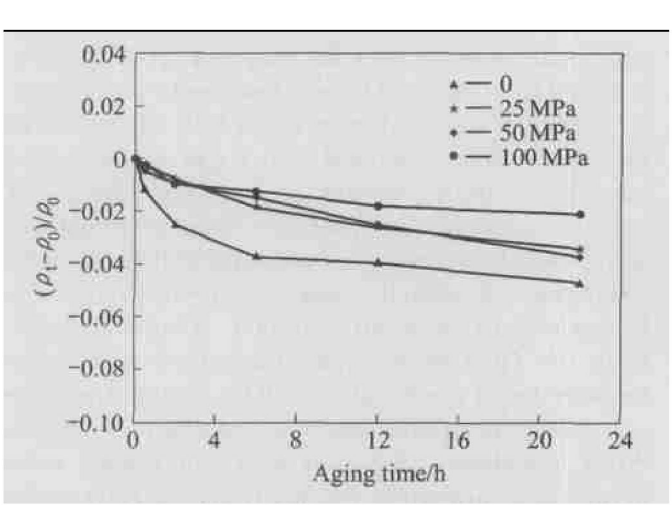

Fig. 1 Curves of relative electrical resistivity vs aging time for Al-Cu binary alloy aged at 180 ℃ under different external stresses after solid solution treatment at 520 ℃, 1 h and WQ (ρ_0—Resistivity in solution-treated stage; ρ_t—Measured instant resistivity)

Fig. 2(a) shows the evolution of the relative resistivity of Al-Cu-Mg-Ag alloy aged at 180 ℃ with respect to aging time during stress aging. It can be found that a peak value exists in each curve which means GP zones or clusters can be found at this time according to the rule of the variation of resistivity. The addition of small amounts of Mg and Ag into Al-Cu alloy with high mass ratio of Cu to Mg will modify the sequence of precipitation and induce a precipitation of Ω phase of disc shape on {111} planes rather than on {001} planes. Suh and Park[13] calculated that the addition of Mg and Ag into Al-Cu alloy induced Mg clusters or Mg-Ag co-clusters on {111} planes, which gives rise to minimum strain energy on {111} planes, therefore, it can be believed that these clusters could be mainly responsible for the formation of Ω phase in Al-Cu-Mg-Ag alloy. This prediction is confirmed by a recent result of atom probe of Ringer et al[14]. They observed that Mg-Ag co-clusters occurred first during artificial aging without well-defined shape. As Cu-atoms assemble to these co-clusters, they start to grow on {111} planes and their shape becomes platelet. These precipitates are designated as {111} GP zones. These plate-like particles on matrix {111} planes grow towards the lateral directions by subsequent aging and start having structural features as the Ω phase. Therefore, the GP zones or clusters as mentioned above are actually Mg clusters or Mg-Ag clusters or {111} GP zones etc.

Comparing Figs. 2(a) with (b), it can be concluded that the variation of relative resistivity as time can be divided into three stages. In the first stage the increasing resistivity corresponds to the formation of clusters/co-clusters or {111} GP zones; in the second stage the decreasing resistivity corresponds to the precipitation of Ω phase; in the third stage the gradual changing resistivity corresponds to the stable existence of Ω phase (because Ω phase has excellent thermal stability at temperatures up to 200 ℃[15, 16]). It

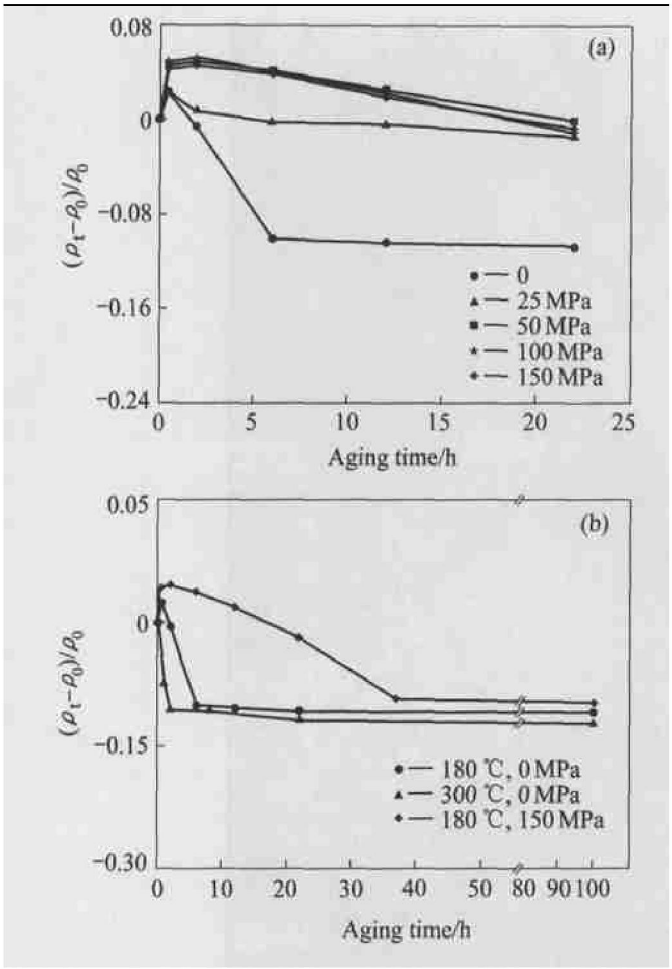

Fig. 2 Curves of relative electrical resistivity vs aging time for Al-Cu-Mg-Ag quaternary alloy under different conditions
(a) —180 ℃ with different external stress;
(b) — Different temperature with different external stress

can be found from Fig. 2(a) that a higher peak value is detected in the relative resistivity curves and that the evolution patterns of the resistivity curves are perfectly similar when the external stress is equivalent to or more than a critical value (50 MPa). These phenomena are attribute to the more formation of clusters/co-clusters or {111} GP zones in the matrix due to the external stress equivalent to or more than threshold value. The decreasing resistivity is due to the precipitation and growth of Ω phases. Compared with the resistivity of normal aging, the decreasing of the resistivity of stress aging is slow, which means that external stress will retard the precipitation and growth of Ω phases.

In order to confirm the above conclusions, we continue to increase aging time to measure the resistivity with external stress equivalent to 150 MPa. Fig. 2(b) shows the evolution of the relative resistivity with respect to the longer aging time at 180 ℃ or 300 ℃ by stress aging or non-stress aging. As mentioned above, if we increase the aging time, it is find that the platform of the resistivity curves also occur during stress aging and the value corresponding to the platform is similar to that of non-stress aging. Therefore, compared with the relative resistiviy of non-stress aging, we can get that the external stress can promote the formation of clusters but retard the precipitation of Ω phases in Al-Cu-Mg-Ag alloy. Another point should be taken care is that the relative resistivity at 300 ℃ aging which do not have obvious peak value in the relative resistivity curve, is completely different to that at 180 ℃. This may be due to clusters or {111} GP zones dissolving or directly precipitating of Ω phases at higher temperature.

TEM micrographs and corresponding SAED patterns of Al-Cu and Al-Cu-Mg-Ag specimens of stress aging or non-stress aging to peak values are shown in Fig. 3.

Three different variants of θ′-phase in Al-Cu alloy are precipitated in {100} planes with equiprobability(Fig. 3(a)). One of the θ′ variants is invisible due to its orientation paralleling to the electronic beam. Contrary to the non-stress aging specimens, in which three types of θ′ variants are equally present, the stress aging specimens show the preferential formation of particular variants of θ′(Fig. 3(b)). Figs. 3(c)-(f) show a series of bright field (BF) TEM images taken from [001] and [110] zone axes of Al-Cu-Mg-Ag alloy respectively, and corresponding selected area electronic diffraction patterns (SAED). The presence of Ω phase is characterized based on diffraction spots at (1/3){022} and (2/3){022} as seen in Figs. 3(c)-(f). Fig. 3(c) shows the perpendicular precipitates of θ′. Many of them are precipitated on the dislocations. Compared with Fig. 3(c), the precipitates are not perpendicular again in Fig. 3(d). It may be due to the orientation of θ′ modified by the external stress since not new diffraction spots are found in the SAED patterns. The above conclusion is inconclusive, however, we still need more experiments to confirm it. The homogeneous distribution of Ω phases and a small amount perpendicular θ′ phases can be seen in Fig. 3(e). Streaks along ⟨111⟩ directions are from the plate-like precipitates on {111} planes, and those along ⟨100⟩ directions are from the GP zones or θ″ on the {100} planes. Although the SAED pattern in Fig. 3(f) is similar to that in Fig. 3(e), the prefertial formation of particular variants of (111) Ω can be observed in Fig. 3(f). It is worth to point out that the prefernetial formation of particular variants of precipitates in Al-Cu-Mg-Ag alloy is not more complete than that in Al-Cu binary alloy. More-

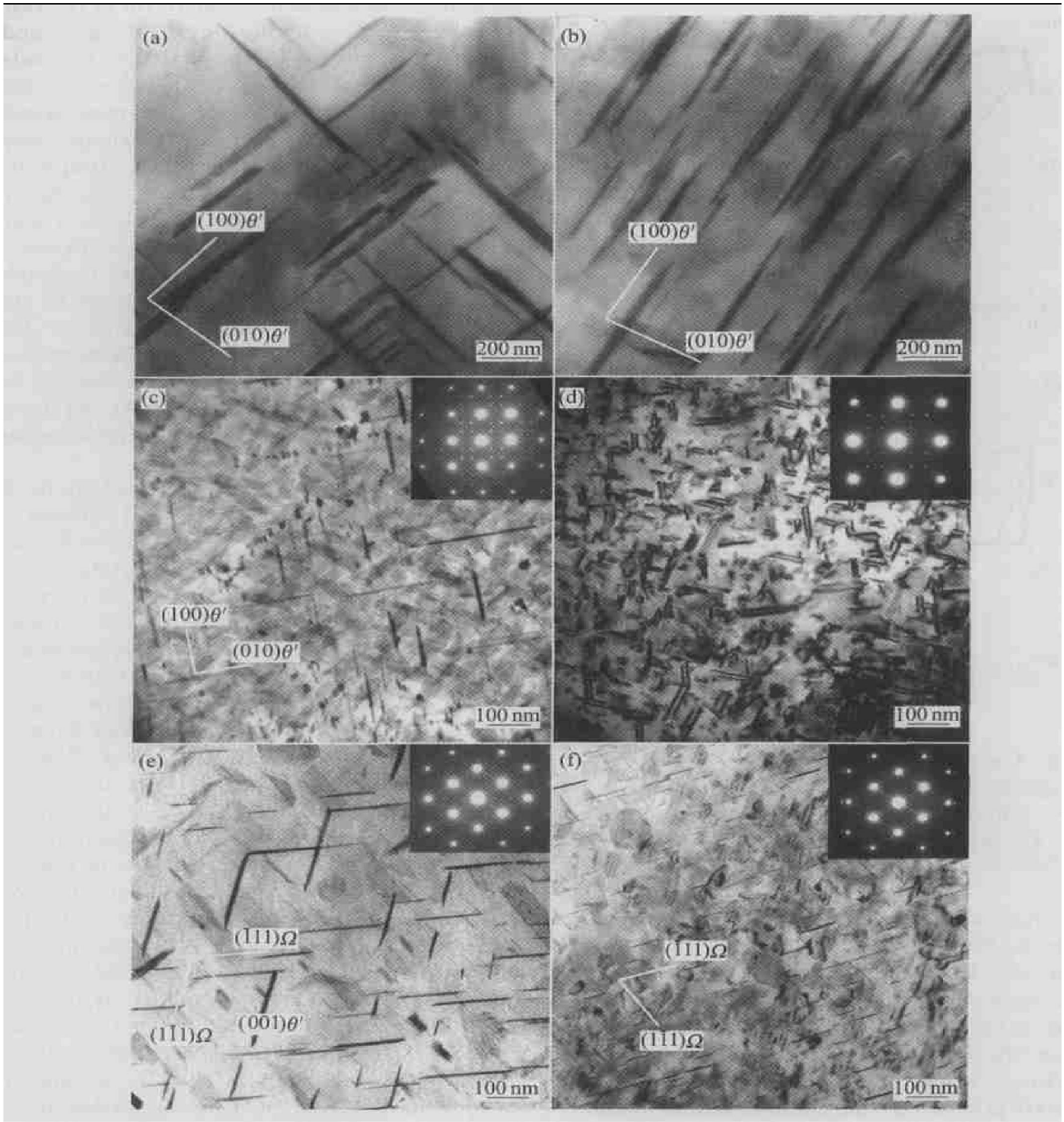

Fig. 3 Bright field TEM images and corresponding SAED patterns of Al alloys under different thermal treatment conditions

(a) —Al-Cu: 0 MPa, 32 h, 180 ℃, θ′ perpendicular to each other, electron beam close to [001];
(b) —Al-Cu: 80 MPa, 32 h, 180 ℃, θ′ prefertially oriented, electron beam close to [001];
(c) —Al-Cu-Mg-Ag: 0 MPa, 8 h, 180 ℃, θ′ perpendicular to each other, electron beam close to [001];
(d) —Al-Cu-Mg-Ag: 120 MPa, 8 h, 180 ℃, showing changes for θ′ under stress, electron beam close to [001];
(e) —Al-Cu-Mg-Ag: 0 MPa, 8 h, 180 ℃, showing two variants of Ω and θ′, electron beam is close to [110];
(f) —Al-Cu-Mg-Ag: 120 MPa, 8 h, 180 ℃, showing stress orienting effect, electron beam close to [110]

over, contrary to the free aging specimens, the stress aging specimens show the smaller and more homogeneous distribution of Ω phases, which makes it possible to improve the mechanical property of Al-Cu-Mg-Ag alloys and also confirms the above experiment results of resisitivity measurement.

Although the value of the applied stress in Al-Cu-Mg-Ag alloy is much more than that in Al-Cu alloy, the stress-induced orientation effect is not obvious, which is in agreement with the experimental results of Skrotzki et al[5]. They suggested that the different misfit strains (experiments have determined

that Ω has a large negative misfit of – 9.3%[17] or – 8.3%[18], and is twice as high as that of θ′) and the different habit planes between Ω and θ′ required a higher stress to induce the stress-induced orientation effect of quarternary alloy than that of binary alloy.

4 THEORETICAL CALCULATION AND ANALYSIS

With the assumption of the direct precipitating of θ′ from the matrix, in this experiment the Eshelby elastic inclusion theory[19, 20] is employed to analyze the reason of stress-induced orientation effect. The precipitation of coherent or semi-coherent second phases is determined by the misfit strain between the second phase and the matrix. The strain field of coherent or semi-coherent second phases can be decreased or increased due to the interaction between applied stress and misfit strain. The interaction energy can, in the terminology of continuum mechanics by Eshelby, be expressed as the modulus effect E_1 due to the difference of the elastic modulus and the the misfit effect E_2 due to the presence of misfit strain $\varepsilon_{ij}^{T^*}$ (stress free transformation strain or eigenstrain) between the matrix and second phase. They are calculated as

$$E_1 = - V\sigma_{ij}^{A}\varepsilon_{ij}^{*}/2 \quad (1)$$

$$E_2 = - V\sigma_{ij}^{A}\varepsilon_{ij}^{T} \quad (2)$$

where V is the volume of the particles, σ_{ij}^{A} the applied stress and ε_{ij}^{*} and ε_{ij}^{T} are, respectively, defined by

$$C_{pqik}(e_{ik}^{A} + S_{ikmn}\varepsilon_{mn}^{*} - \varepsilon_{ik}^{*}) = C_{pqik}^{*}(e_{ik}^{A} + S_{ikmn}\varepsilon_{mn}^{*}) \quad (3)$$

$$C_{pqik}(S_{ikmn}\varepsilon_{mn}^{T} - \varepsilon_{ik}^{T}) = C_{pqik}^{*}(S_{ikmn}\varepsilon_{mn}^{T} - \varepsilon_{mn}^{T^*}) \quad (4)$$

where $e_{ik}^{A} = C_{ikjl}^{-1}\delta_{jl}^{A}$ and S_{ikmn} is the Eshelby tensor, C_{pqik} and C_{pqik}^{*} are the elastic constants of the matrix and the second phase, respectively. In the case of the cubic crystal system, the Eshelby tensor of different morphologies of second phases can be found. With Eqns. (1), (2) and (3), it is apparent that the modulus effect has the quadratic form of the applied stress and is independent on the misfit strain of second phases. Thus, the modulus effect does not induce the stress-induced orientation effect.

The eigenstrain can be calculated by the lattice parameters of θ′ ($a = b = 0.404$ nm, $c = 0.580$ nm) and the matrix ($a = b = c = 0.404\ 9$ nm). The eigenstrain is thus represented as

$$\varepsilon_{11}^{T^*} = \varepsilon_{22}^{T^*} = - 0.002\ 2,\ \varepsilon_{33}^{T^*} = - 0.045,\ \varepsilon_{ij}^{T^*} = 0 (i \neq j)$$

On the assumption that the applied stress along Z axis has the same direction as C axis of crystal, the misfit strain energy of the precipitates in unit volume, lying perpendicular to and parallel to the stress axis (see Fig. 4), e_{I}^{e} and e_{II}^{e}, with the applied stress, $\sigma^{A} = \sigma_{33}^{A} = 80$ MPa, is calculated as

$$e_{\mathrm{I}}^{e} = - \sigma^{A}\varepsilon_{33}^{T} \quad (5)$$

$$e_{\mathrm{II}}^{e} = - \sigma^{A}\varepsilon_{11}^{T} \quad (6)$$

Using the elastic constants of pure aluminium and θ′:

$C_{1111} = C_{11} = 108.2$ GPa, $C_{1122} = C_{12} = 61.3$ GPa, $C_{2323} = C_{44} = 29.0$ GPa

$C_{1111}^{*} = C_{11}^{*} = 138.3$ GPa, $C_{1122}^{*} = C_{12}^{*} = 91.4$ GPa, $C_{2323}^{*} = C_{44}^{*} = 39.4$ GPa

Then

$$\varepsilon_{11}^{T} = 1.088\,\varepsilon_{11}^{T^*} \quad (7)$$

$$\varepsilon_{33}^{T} = 0.085\,\varepsilon_{11}^{T^*} + \varepsilon_{33}^{T^*} \quad (8)$$

With Eqns. (5)–(8), we can get: $e_{\mathrm{I}}^{e} = 36.15$ J/m^3, $e_{\mathrm{II}}^{e} = 1.91$ J/m^3.

Therefore, the systematic strain energy will be increased under tensile stress. It is found that the increasing of the strain energies of variant 1 is much more than that of variant 2 and thus variant 2 will preferentially precipitate at the cost of variant 1. The stress-induced orientation effect can also be predicted under tensile stress. What is different is that the systematic strain energy will be decreased at different extents.

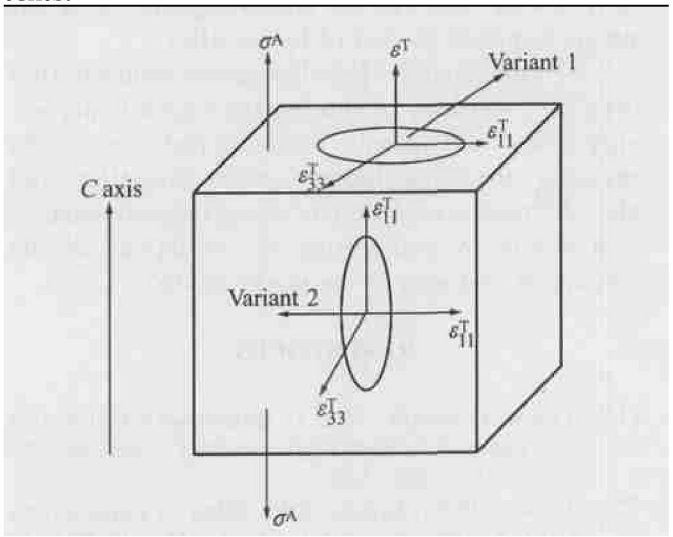

Fig. 4 Scheme of external stress applied to two variants

The reason of different experimental results from different authors[2, 3] can be explained by using the above analysis. On taking a close look at the eigenstrain of θ′ phase, one can see that the major component of the eigenstrain is a negative misfit strain along Z direction. This negative eigenstrain causes a tensile strain along the Z direction. If a compressive external strain is applied along the Z axis, it reduces this internal tensile strain and thus decreases the strain energy barrier to the growth of the precipitate which lies perpendicular to the compressive stress. If a tensile

stress is applied, however, it will increase this tensile strain and thus unfavors the growth of the precipitate. As a result only those variants which lie along tensile applied stress will grow selectively. Therefore, the contradiction of different conclusions by different authors can be explained from possible variations in the lattice misfit. For example, as suggested, small θ′ precipitates have a negative misfit. While this misfit may change its sign and magnitude during particle growth. The variation of misfit strain can naturally affect the interaction energy and then induce the different stress-induced orientation effects.

5 CONCLUSIONS

1) After stress aging at 180 ℃, the precipitation and growth of θ′/θ″ are retarded for Al-Cu binary alloy and the formation of Mg clusters or Mg-Ag co-clusters or {111} GP zones is promoted and the growth of Ω are also retarded for Al-Cu-Mg-Ag quartnertary alloy.

2) With applied stress of 80 MPa, the preferential formation of θ′ is observed after being aged at 180 ℃ for about 32 h for Al-Cu alloys. With applied stress of 120 MPa, the preferential formation of Ω is also observed for Al-Cu-Mg-Ag alloys but not as complete as that of binary alloys.

3) Calculated by Eshelby elastic inclusion theory, the variations of the system elastic strain energy of different variants under applied stress is the reason of the stress-induced orientation effect and also the reason of different stress-induced orientation effects by considering the variations of the magnitude and sign of the misfit strain.

REFERENCES

[1] Tanaka Y, Sato A, Mori T. Stress assisted nucleation of precipitates in Fe-N single crystal[J]. Acta Metall, 1978, 26(4): 529-540.

[2] Hosford W F, Agrawal S P. Effect of stress during aging on the precipitation of in the Al-4wt% Cu[J]. Metall Trans, 1975, 6A(3): 487-491.

[3] Eto T, Sato A, Mori T. Stress-oriented precipitation of G.P. zones in Al-Cu alloy[J]. Acta Metall, 1978, 26(3): 499-508.

[4] Zhu A W, Starke E A Jr. Precipitation strengthening of stress-aged Al-xCu alloys[J]. Acta Mater, 2000, 48(9): 2239-2246.

[5] Skrotzki B, Shiflet G J, Starke E A Jr. On the effect of stress on nucleation and growth of precipitates in an Al-Cu-Mg-Ag alloy[J]. Metall Mater Trans, 1996, 27A(11): 3431-3444.

[6] Zhu A W, Starke E A Jr. Stress aging of Al-xCu alloys: experiments[J]. Acta Mater, 2001, 49(12): 2285-2295.

[7] Nishizawa H, Sukedai E, Liu W, et al. Effect of applied stress on formation of w-phase in Ti alloys[J]. Mater Trans JIM, 1998, 39(5): 609-612.

[8] Mukhopadhyay A K, Murken J, Skrotzki B, et al. Nature of precipitates in peakaged and in subsequently crept Al-Ge-Si alloy[J]. Mater Sci Forum, 2000, 331-337: 1555-1560.

[9] Li D Y, Chen L Q. Computer simulation of stress oriented nucleation and growth of precipitates in Al-Cu alloys[J]. Acta Mater, 1998, 46(8): 2573-2585.

[10] Rossiter P L. The Electrical Resistivity of Metals and Alloys[M]. Cambridge University Press, 1987. 257-261.

[11] Hull S, Messoloras S, Stewart R J. Study of theta prime precipitates in an Al-1.56 at% Cu single crystal using electrical resisitivity, small-angle neutron scattering and hardness measurements[J]. Philosophical Magazine A, 1988, 57(2): 261-276.

[12] Suh I S, Park J K. Influence of the elastic strain energy on the nucleation of Ω phase in Al-Cu-Mg(-Ag) alloys[J]. Scripta Metallurgica et Materialia, 1995, 33(2): 205-211.

[13] Reich L, Murayama M, Hono K. Evolution of Ω phase in an Al-Cu-Mg-Ag alloy—a three-dimensional atom probe study[J]. Acta Mater, 1998, 46(17): 6053-6062.

[14] Huchinson C R, Fan X, Pennycook S J, et al. On the origin of the high coarsening resistance of Ω plates in Al-Cu-Mg-Ag alloys[J]. Acta Mater, 2001, 49(14): 2827-2841.

[15] Ringer S P, Yeung W, Muddle B C, et al. Precipitate stability in Al-Cu-Mg-Ag alloys aged at high temperatures[J]. Acta Metall Mater, 1994, 42(1-4): 1715-1725.

[16] Fonda R W, Cassada W A, Shiflet G J. Accommodation of the misfit strain surrounding {111} precipitates (Ω) in Al-Cu-Mg-(Ag)[J]. Acta Metall Mater, 1992, 40(10): 2539-2546.

[17] Eshelby J D. The determination of the elastic field of an ellipsoidal inclusion, and related problems[J]. Proc R Soc A, 1957, 241. 376-396.

[18] Eshelby J D. The elastic field outside an ellipsoidal inclusion[J]. Proc R Soc A, 1959, 252. 561-569.

[19] Eshelby J D. Elastic inclusions and inhomogneities[J]. Prog Solid Mech, 1961, 2. 87-140.

[20] Stobbs W M, Purdy G R. The elastic accommodation of semicoherent phase in Al-4wt% Cu alloy[J]. Acta Metall, 1978, 26(7): 1069-1081.

(Edited by LONG Huai-zhong)